

This discussion paper is/has been under review for the journal Hydrology and Earth System Sciences (HESS). Please refer to the corresponding final paper in HESS if available.

# Applying a time-lapse camera network to observe snow processes in mountainous catchments

J. Garvelmann, S. Pohl, and M. Weiler

Institute of Hydrology, Freiburg, Germany

Received: 5 September 2012 – Accepted: 13 September 2012  
– Published: 20 September 2012

Correspondence to: J. Garvelmann (jakob.garvelmann@hydrology.uni-freiburg.de)

Published by Copernicus Publications on behalf of the European Geosciences Union.

HESSD

9, 10687–10717, 2012

Applying  
a time-lapse camera  
network to observe  
snow processes

J. Garvelmann et al.

Title Page

Abstract

Introduction

Conclusions

References

Tables

Figures

◀

▶

◀

▶

Back

Close

Full Screen / Esc

Printer-friendly Version

Interactive Discussion

## Abstract

A network of 45 spatially distributed time-lapse cameras was used to carry out a continuous observation of snow processes and snow cover properties throughout three mid-latitude medium elevation mountain catchments in hourly intervals. A simple technical modification was conducted to enable the deployment of the standard digital cameras in any location. Image analysis software was applied to extract information about snow depth, surface albedo, and canopy interception from the digital images. Furthermore, the distributed design of the camera network made it possible to identify the elevation of the snow rain interface for any precipitation event for the interpretation of winter flooding events resulting from snow melt. Study results prove that the application of digital time-lapse photography is an appropriate technique to observe the spatial distribution and temporal evolution of seasonal snow covers in a mountainous environment.

## 1 Introduction

Snow is an important component of the hydrological system in many mountainous environments. Vegetation and topography have a crucial influence on the spatial distribution and temporal evolution of snow covers and the relation of all factors influencing the distribution have not been well understood (e.g. Jost et al., 2007, 2009). A continuous monitoring of the snow cover at the catchment scale is valuable to improve the understanding of the processes driving the spatio-temporal variability of seasonal snow covers. Furthermore, it yields important information for water resource applications and the prediction of snow melt runoff events. The interception of snow in the forest canopy is a major factor contributing to the difference in snow accumulation between open and forested areas (Hedstrom and Pomeroy, 1998; Storck et al., 2002). Different processes (mass unload, sublimation, and melt water drip) are involved in the unloading of snow from the canopy (Pomeroy et al., 1998). Incoming global radiation is often the most important component of the snowmelt energy balance. The albedo of the snow surface

## Applying a time-lapse camera network to observe snow processes

J. Garvelmann et al.

<a href="#">Title Page</a>	
<a href="#">Abstract</a>	<a href="#">Introduction</a>
<a href="#">Conclusions</a>	<a href="#">References</a>
<a href="#">Tables</a>	<a href="#">Figures</a>
<a href="#">◀</a>	<a href="#">▶</a>
<a href="#">◀</a>	<a href="#">▶</a>
<a href="#">Back</a>	<a href="#">Close</a>
<a href="#">Full Screen / Esc</a>	
<a href="#">Printer-friendly Version</a>	
<a href="#">Interactive Discussion</a>	

**Applying  
a time-lapse camera  
network to observe  
snow processes**

J. Garvelmann et al.

describes the fraction of absorbed shortwave radiation therefore strongly influencing the energy balance in snowmelt. Snow albedo values decrease after a fresh snowfall mostly due to metamorphic snow processes. During the metamorphose snow grain sizes are increasing resulting in a decreasing albedo (Wiscombe and Warren, 1980).  
5 In addition, particles (aerosols, dust, needles and small branches) falling on the snow are also contributing to a decrease of snow surface albedo (Warren and Wiscombe, 1980; Hardy et al., 2000; Melloh et al., 2001). Different albedo decay functions have been used so far in modeling snowmelt (e.g. Gray and Landine, 1987; Link and Marks, 1999; Garen and Marks, 2005; Pomeroy et al., 2007; Mazurkiewicz et al., 2008). Jost  
10 et al. (2009) observed that the shape of the predicted albedo decay is generally too steep. They used different albedo decay functions for forested and open sites that were derived by fitting to observed albedo values in order to calculate realistic snow ablation rates.

Manual snow surveys have been used in various studies to measure the evolution  
15 of the snow pack (e.g. Stottlemeyer and Troendle, 2001; Lundberg and Koivusalo, 2003; Winkler et al., 2005; Jonas et al., 2009). Continuous observations at the catchment scale are missing and therefore event based analysis of snow cover properties and snow processes is often not possible.

Terrestrial time-lapse photography is a non-destructive method and, compared to  
20 satellite remote sensing techniques, it is relatively economic and allows for a high spatial and temporal resolution. In snow research, time-lapse photography has been used to observe the distribution and patterns of snow covers (e.g. Hinkler et al., 2002; Farinotti et al., 2010). Floyd and Weiler (2008) have shown that time-lapse photography is an appropriate technique for an event based analysis of accumulation and  
25 ablation of snow, interception of snow in the forest canopy and subsequent unloading. Furthermore they used the images to monitor the state of precipitation. Parajka et al. (2012) showed the potential of time-lapse photography for the observation of the spatio-temporal variability of snow depth and interception in the near range (100–300 m) and snow cover patterns in the far range (ca. 1000–2000 m) of the camera

[Title Page](#)[Abstract](#)[Introduction](#)[Conclusions](#)[References](#)[Tables](#)[Figures](#)[Back](#)[Close](#)[Full Screen / Esc](#)[Printer-friendly Version](#)[Interactive Discussion](#)

view, respectively. An overview of studies using time-lapse photography in glaciology and snow research can be found in Parajka et al. (2012).

In this study we further extend these approaches by modifying standard digital cameras to run independently of any outside stationary power source. This allowed us to set up an experimental design consisting of a network of numerous standard standalone digital time-lapse cameras distributed throughout the study watersheds and covering a wide variety of topographical and vegetational situations. In addition, we automated and extended the information that can be derived from the time-lapse images to derive time series of snow depth, albedo, snow interception, and the state of precipitation.

## 10 2 Methodology

### 2.1 Study area and camera network

The study was conducted in the Black Forest, a typical mid latitude medium elevation mountain range in the southwest of Germany. In order to accomplish a continuous observation of the quantity and the status of the snow cover, a network of 15 standalone digital time-lapse cameras was established over the winter season 2010/2011 in a meso scale catchment. The network was extended to 45 cameras spread over three watersheds of different sizes and topographic characteristics for the 2011/2012 winter (Fig. 1).

Within the study catchments, a stratified sampling design was used to cover a wide range of altitudes and exposures. To specifically investigate the influence of the vegetation cover on the accumulation and ablation processes of the snowpack beneath, generally pairs of cameras were installed in close proximity to each other with one being located underneath the forest canopy while the other was situated on an adjacent open field site.

[Title Page](#)

[Abstract](#)

[Introduction](#)

[Conclusions](#)

[References](#)

[Tables](#)

[Figures](#)

◀

▶

◀

▶

[Back](#)

[Close](#)

[Full Screen / Esc](#)

[Printer-friendly Version](#)

[Interactive Discussion](#)

## 2.2 Camera design

We used a standard “Pentax Optio W90” digital camera, which is a waterproof outdoor camera. The camera is equipped with a 12 megapixel 1/2.3" RGB-CCD-sensor chip and allows to electronically set-up a time-lapse routine. Hourly pictures were stored on a camera internal 2 GB SD-card. The time-lapse mode of the camera allows for a maximum of 1000 images. Therefore the cameras had to be read-out and restarted after a maximum duration of 41 days. To ensure a continuous power-supply for the digital camera, we used a 3.7 V external rechargeable Lithium-Polymer battery. Rechargeable Lithium-Polymer batteries are known to provide reliable power supply even for low temperatures. Cables were soldered to the camera internal battery terminals which we connected with gold plated plugs to the rechargeable Lithium-Polymer batteries (Fig. 2). With this modification we were able to install and run the digital cameras independently of any additional power source at any location in the field. This gave us complete freedom to choose adequate locations to suit our research questions. It also made the installation comparably easy and time efficient, which was essential for setting up the high density camera network used in this study. To protect the cameras from severe weather conditions and minimize drops on the camera lens, they were mounted within wooden birdhouses, which were then mounted to trees and other suitable objects in the field (Fig. 2). The birdhouses also helped us to reduce vandalism of the equipment in the watersheds.

## 2.3 Image analysis

We used IDL image processing software to extract information about snow depth, albedo and the interception of snow in the forest canopy from the digital images. A wooden measurement stake with alternating 10 cm black and red bars was installed in camera view at every location to accommodate the snow depth estimation. On top of the stake a black/white plastic board was attached to provide a control surface of a “perfect white and black” area for each picture. Having these boards in the pictures

[Title Page](#)

[Abstract](#)

[Introduction](#)

[Conclusions](#)

[References](#)

[Tables](#)

[Figures](#)

◀

▶

◀

▶

[Back](#)

[Close](#)

[Full Screen / Esc](#)

[Printer-friendly Version](#)

[Interactive Discussion](#)



## Applying a time-lapse camera network to observe snow processes

J. Garvelmann et al.

allows the direct determination of the references for black and white for differing illumination conditions in the image analysis. A white balance was used for the albedo estimation and a black/white balance for the calculation of canopy interception. Polygon masks, called regions of interest (ROI), were defined within each image to define the areas within the pictures for which snow surface albedo and canopy interception calculations were carried out (Fig. 3). Several ROIs for albedo or interception analysis can be defined within the pictures providing more representative average values for a location but also allowing an analysis of the potential variability of those values at a location.

A batch analysis routine was used to load and analyze each image. RGB values for every pixel within the defined polygon masks and the control surfaces (black/white board) are used for the calculations. The calculated output was written to a text file which could be used for further analysis. Images taken at night and during poor visibility conditions (fog, intense snowfall events) were discarded and could not be used for the image analysis resulting in data gaps.

The established camera network allowed a continuous observation of snow depths at different locations throughout the catchments. These snow depth time series and accompanying snow surveys which determined snow densities can be used to calculate snow water equivalents (SWE). Snow depth can be calculated automatically with image analysis software from the images by counting the number of snow stake pixels not covered with snow (Floyd and Weiler, 2008; Parajka et al., 2012). Such a computer routine was applied to calculate the snow depth at the camera locations. To check the accuracy of this automated process we also determined the snow depths “manually” by opening each picture and determining the snow depth by counting the visible red and black bars by eye. Figure 4 shows the comparison of the two methods for one location ( $R^2 = 0.98$ , RMSE = 7.1 cm). The comparison shows that the overall evolution of the snow depth over the winter is reproduced well by the automated method. However, there seems to be a constant slight underestimation of snow depths at higher values.

<a href="#">Title Page</a>	
<a href="#">Abstract</a>	<a href="#">Introduction</a>
<a href="#">Conclusions</a>	<a href="#">References</a>
<a href="#">Tables</a>	<a href="#">Figures</a>
<a href="#">◀</a>	<a href="#">▶</a>
<a href="#">◀</a>	<a href="#">▶</a>
<a href="#">Back</a>	<a href="#">Close</a>
<a href="#">Full Screen / Esc</a>	
<a href="#">Printer-friendly Version</a>	
<a href="#">Interactive Discussion</a>	

We therefore chose to “manually” determine the snow depths from the digital images for this study.

The snow surface albedo estimation from the images is limited by the fact, that the CCD-sensor used in the digital cameras is only able to detect the visible range of the electromagnetic spectrum. Therefore we can only estimate the snow surface albedo within the visible range. Nevertheless, Corripio (2004) has shown that terrestrial photography is a suitable and useful approach to estimate snow surface albedo. He used an algorithm for georeferencing the images in order to correct the reflectance values of the images with respect to the topographic position. In this study we used an even simpler approach by Gorski (2011) to estimate albedo values directly from digital images. The calculated albedo value is the ratio of the mean RGB pixel values of a control surface (white board in the focus of the camera) and the mean RGB pixel value of defined polygon masks on the snow surface within the digital image. The computed ratio is adjusted with a correction factor of 0.6 which Gorski (2011) suggest is suitable for CCD-sensor cameras. The albedo is therefore calculated as follows:

$$\text{Albedo} = 0.6 \times (\overline{\text{RGB}}_{\text{snow}} / \overline{\text{RGB}}_{\text{reference}}) \quad (1)$$

$\overline{\text{RGB}}_{\text{snow}}$  = mean of the RGB pixel values in the ROI on the snow surface

$\overline{\text{RGB}}_{\text{reference}}$  = mean of the RGB pixel values of the reference area

For the calculation of snow interception in the forest canopy we first performed a black/white balance using the control surfaces mounted on top of the snow stakes in the images. Based on this balance white (snow) pixels could then be distinguished from non-white (non-snow) pixels within the polygon masks and a fraction of snow (white pixels) could be calculated. A fraction of zero would therefore indicate no snow in the canopy and a fraction of one would indicate a completely snow covered canopy, respectively. It is important to note that the fraction of white pixels within the defined ROI depends on the camera position, view angle and distance of the camera to the

## Applying a time-lapse camera network to observe snow processes

J. Garvelmann et al.

[Title Page](#)

[Abstract](#)

[Introduction](#)

[Conclusions](#)

[References](#)

[Tables](#)

[Figures](#)



[Back](#)

[Close](#)

[Full Screen / Esc](#)

[Printer-friendly Version](#)

[Interactive Discussion](#)

## Applying a time-lapse camera network to observe snow processes

J. Garvelmann et al.

[Title Page](#)

[Abstract](#)

[Introduction](#)

[Conclusions](#)

[References](#)

[Tables](#)

[Figures](#)



[Back](#)

[Close](#)

[Full Screen / Esc](#)

[Printer-friendly Version](#)

[Interactive Discussion](#)

canopy. Therefore, this method initially only provides relative values for the total snow load within the forest canopy.

The images could also be used to identify the state of precipitation at the camera locations. Since the digital time-lapse cameras were deployed at different altitudes, the images could therefore be used to determine elevation ranges for the snow line during different winter precipitation events.

### 3 Results

#### 3.1 Snow depth

Figure 5a shows the snow depth at three open and one forest location of similar exposition but different elevation. As expected the snow depths increase with increasing elevation at the open locations. It is interesting to note that the snow depths at the peak of the snowpack differ by as much as 53 cm (150 mm SWE) between the highest and lowest location. Furthermore, the analysis shows that the snow cover duration was about 16 days shorter for the 2011/2012 winter for the 900 m a.s.l. location compared to the 1200 m a.s.l. location. A comparison with the fourth location, which was situated underneath a dense forest canopy at an elevation of 1195 m a.s.l. highlights the strong effect a forest canopy has on the snow cover distribution in watersheds. A difference of 55 cm (155 mm SWE) was observed for peak snow depth (around 22 February 2012), while in the spring the ground underneath the forest first became snow free 27 days before the snow on the adjacent open meadow disappeared.

Figure 5b presents the snow depths during the winter 2011/2012 at four different locations at similar elevation but different expositions and land cover. The influence of the exposition can be clearly seen for the two open locations with a significantly deeper snowpack on the north-facing slope. The overall maximum difference in snow depth between the two open locations is about 30 cm (or about 90 mm SWE). The observed snow depths at the two forest locations are nearly identical suggesting that exposition

does not play an important role for snow accumulation under forest canopies. The results, however, once again shows the great importance the forest cover has on the snow cover as there are large differences in snow depth between open and forest locations. Figure 5 also shows the great potential of the camera pairs (open vs. forest locations) used in the current study to investigate the influence of a vegetation cover on the snowpack beneath in considerable detail. Overall, the presented results demonstrate the crucial importance of determining the small scale snow cover variability even in a medium elevation mountain range for a wide variety of hydrologic and ecologic aspects.

Based on the snow depth observations at the 19 camera locations throughout the Brugga watershed and snow density measurements from manual snow surveys, the spatial distribution of the SWE in the Brugga catchment prior to and after a rain-on-snow event on 2 January 2012 was determined using a simple linear regression model (Fig. 6). Elevation was related to snow depth separately for open and forested for each time, respectively. Subsequently, SWE was calculated for each  $10 \times 10$  m grid square in the catchment using elevation and land cover data. The flood peak observed on 2 January 2012 (see Fig. 7) was categorized as a 2-yr flood event at the basin outlet. More extreme flood discharges were measured in some of the tributaries. The flood was generated by both liquid precipitation and snow melt water. There was a snow cover present throughout the catchment prior to the event ranging from a few cm in the lowest parts to more than 50 cm in the highest parts of the catchment. Snow depths and consequently SWE decreased significantly at all altitudes during this ROS event. With the linear regression model a basin wide mean SWE of 56 mm was calculated for the snow cover prior to the event, whereas a mean SWE of 13 mm was determined for the snow cover after the event. Therefore, a total of 43 mm of SWE melted during the event. Total precipitation was 44 mm during this event. Assuming a negligible change in storage within the catchment these input values ( $43\text{mm} + 44\text{mm} = 87\text{mm}$ ) match the observed total runoff of 83 mm very well. The numbers also show the importance of

## Applying a time-lapse camera network to observe snow processes

J. Garvelmann et al.

[Title Page](#)

[Abstract](#)

[Introduction](#)

[Conclusions](#)

[References](#)

[Tables](#)

[Figures](#)

◀

▶

◀

▶

[Back](#)

[Close](#)

[Full Screen / Esc](#)

[Printer-friendly Version](#)

[Interactive Discussion](#)

the snowmelt for this flood event as about half of the available flood peak input resulted from the rain-on-snow melt of the pre-existing snow cover.

Subsequently, the time-lapse images from different locations throughout the catchment were used for a further detailed interpretation of the hydrograph for this and a subsequent runoff event 2 days later (Fig. 7). Despite higher precipitation intensity and amount the flood peak was slightly lower. The pictures show that most snow in the catchment had disappeared during the rain-on-snow event on 2 January 2012. Therefore the water available for runoff during this event was virtually limited to rainwater and, as a result, discharge did not rise as high. Another precipitation event (6 January 2012) caused nearly no runoff increase, because as the pictures indicate, precipitation fell as snow in most parts of the catchment.

### 3.2 Snow canopy interception

The experimental setup presented in this study allows a continuous observation of the forest canopy and the temporal evolution of the snow interception in the canopy at different topographic situations and during various climatic conditions. Figure 8 shows the snow interception results obtained from images taken by a camera installed at 900 m a.s.l. altitude and a viewing direction of north-east. Daily interception values from the beginning of December 2011 through end of February 2012 are shown. Several snowfall events could be observed during this period. Events of particular interest are labeled with red arrows and the corresponding pictures after the snowfall events are shown. It is interesting to note, that more snow was intercepted in the canopy on 20 December 2011 compared to 15 February 2012 even though more snow fell on 15 February. The reason is most likely the difference in air temperatures during the events. Average daily temperature on the 19 and 20 December 2011 were much higher at 1.5 °C compared to –5.5 °C in February 2012. Previous studies have suggested that interception efficiency increases with decreasing density of the falling snow, increasing temperature and decreasing wind speed (Pomeroy and Gray, 1995; Marsh, 1999). The warmer temperatures result in more flexible tree limbs and lead to the building of ice bridges

[Title Page](#)[Abstract](#)[Introduction](#)[Conclusions](#)[References](#)[Tables](#)[Figures](#)[◀](#)[▶](#)[Back](#)[Close](#)[Full Screen / Esc](#)[Printer-friendly Version](#)[Interactive Discussion](#)

between the individual needles and snow crystals therefore allowing more snow to be intercepted. The results of this study clearly support this assumption.

The event around 3 February 2012 is special in terms of the snow removal from the canopy. The sublimation or unloading of snow from the canopy was much slower compared to the other events observed. This behavior can most likely be attributed to the meteorological conditions a nearby weather station observed at the time of the event. Air temperatures were consistently below freezing and incoming solar radiation was high during the entire period after the 3 February 2012 event. For the other events shown in Fig. 8, observed air temperature was higher and the radiation energy input was lower. This analysis indicates that sublimation of intercepted snow directly back to the atmosphere dominated this event. This is a much slower process than the mass unload and melt water drip processes, that were most likely responsible for the quick disappearance of the intercepted snow after the other events.

Figure 9 shows the comparison of the snow interception of similar forests on a north-facing versus a south-facing slope for a snowfall event in February 2012 in the Breg catchment. The snowfall event was followed by an overcast day with freezing temperatures where the snow remained in the canopy at both expositions. The following sunny day with moderate temperatures close to 0 °C caused an abrupt decrease in intercepted snow. The comparison shows that the release of the snow interception storage progressed much faster at the southfacing canopy. As a result the forest canopy on the southfacing slope was snow free two days earlier compared to the canopy on the northfacing slope probably due to a more intense input of solar radiation to the south facing slope.

These results indicate the difficulties in modeling the unloading of snow with simple interception models (e.g. Hedstrom and Pomeroy, 1998) in this environment as compared to colder environments where these kinds of studies have so far often been conducted. It also further highlights the importance of having continuous observations in various topographical situations to better understand the relative importance of the involved processes in relation to topography and meteorological conditions.

---

## Applying a time-lapse camera network to observe snow processes

J. Garvelmann et al.

---

[Title Page](#)

[Abstract](#)

[Introduction](#)

[Conclusions](#)

[References](#)

[Tables](#)

[Figures](#)



[◀](#)

[▶](#)

[Back](#)

[Close](#)

[Full Screen / Esc](#)

[Printer-friendly Version](#)

[Interactive Discussion](#)

### 3.3 Albedo

The albedo of a snow cover provides important information about the status of the snow and its temporal evolution is a crucial factor for the energy balance of the snow. Visible albedo was calculated from the digital images. In the visible range measured albedo values of fresh snow are generally high.

Hourly derived albedo values using Eq. (1) are plotted against measured albedo values from a weather station for eight days showing a high correlation of  $R^2 = 0.89$  (Fig. 10). The resulting regression equation of this correlation was used to calibrate the albedo values calculated with Eq. (1) from the digital images in the catchment to receive useful data.

Figure 11 shows the temporal evolution of the albedo obtained from the time lapse images compared to the albedo measured by a weather station at the same location during a rain-on-snow event followed by fresh snow. The decreasing surface albedo during the melting of the snowpack and a subsequent increase of the albedo caused by new snow can be clearly seen in the graph. The obtained results are in very good agreement with the measured albedo values of the on-site weather station ( $R^2 = 0.89$ , RMSE = 0.08, NS-Efficiency = 0.88). This comparison proves the validity of the presented method to obtain meaningful albedo values using the visible range.

Subsequently, the albedo image analysis was applied to images taken at other field sites in the study area. Figure 12 shows calibrated albedo values of the snow surface under a conifer forest canopy for the entire winter 2011/2012. The data clearly shows the expected increase in albedo after snowfall events. Frequently, a further slight increase in the days following a big snowfall event can also be seen. This phenomenon can be attributed to initially intercepted snow falling out of the canopy and onto the snow cover. The subsequent albedo decrease due to snow metamorphism as well as needles, small branches and other debris deposited on the snow cover underneath the canopy is also well reproduced by the data. Such observations are very valuable for the improvement of snowmelt models as many of these models use open field albedo

[Title Page](#)[Abstract](#)[Introduction](#)[Conclusions](#)[References](#)[Tables](#)[Figures](#)[Back](#)[Close](#)[Full Screen / Esc](#)[Printer-friendly Version](#)[Interactive Discussion](#)

values to calculate the snow cover energy balance underneath a forest canopy. This assumption has to be tested as it could potentially lead to significant errors in the simulation of forest snowmelt rates. Data collected with the presented method can be used for such testing and, if necessary, for the formulation of a new model algorithm.

### 5 3.4 State of precipitation

Time-lapse images were also used to identify the state of precipitation during precipitation events. Due to the high number of digital cameras installed at different elevations in the study catchments, the pictures could be used to identify the elevation of the snow line and its changes over time during precipitation events. Since the study also 10 included the installation of a high density meteorological observation network we were able to compare measured temperature profiles to the snow line determined from the images (Fig. 13). For the 13 December 2011 event the snow line determined from the images was between 890 m a.s.l. and 1010 m a.s.l. (red box). For the 27 January 2012 event the snow line was fairly close to the 780 m a.s.l. since we observed a mix of rain 15 and snow in the pictures at this altitude and snowfall was evident in the pictures of the next higher camera station 890 m a.s.l. (green box). For the third event shown here the snow line was lower than the altitude of the lowest digital camera. Therefore we can assume that the precipitation fell as snow in virtually the entire catchment during this event. When comparing the estimated snow lines from the digital images to the 20 observed temperature profiles we can see that the snow line was at an elevation with an air temperature (2 m above ground) of around 3 °C–4 °C for the 13 December 2011 event and around 2 °C for the 27 January 2012 event, respectively. These temperature values are relative high compared to the frequently used threshold temperatures in many hydrological models.

<a href="#">Title Page</a>	
<a href="#">Abstract</a>	<a href="#">Introduction</a>
<a href="#">Conclusions</a>	<a href="#">References</a>
<a href="#">Tables</a>	<a href="#">Figures</a>
<a href="#">◀</a>	<a href="#">▶</a>
<a href="#">◀</a>	<a href="#">▶</a>
<a href="#">Back</a>	<a href="#">Close</a>
<a href="#">Full Screen / Esc</a>	
<a href="#">Printer-friendly Version</a>	
<a href="#">Interactive Discussion</a>	

## 4 Discussion

With a simple technical modification to a standard digital camera, it was possible to establish a cost and time efficient network of time-lapse cameras in several meso-scale mountain catchments to perform a very detailed continuous observation of the snow cover and snow processes. However, there are some limitations concerning this technique. Gaps in the data are caused by: (1) photographs taken during night time which are useless for the analysis; (2) strong snow fall events causing frost or snow to accumulate on the lens of the camera; (3) reduced visibility due to fog and (4) images showing snow rime build up or snow sticking to the measurement scale and the black/white reference scale. These images had to be discarded from the image analysis. Furthermore, the camera locations had to be accessible to download the images three to four times during the winter season. Unfortunately, it is not possible to switch off the camera during night time, which would increase the period between having to download the images significantly. It is also not possible to increase the number of pictures taken by the camera (1000) despite the SD card could store many more pictures.

A fully automated analysis of the digital images was not always possible, since the cameras are moving slightly due to wind or snow on the camera housing and after downloading the images. Further improvements of the image analysis software could account for these limitations for example with an automatic identification of the measurement scales needed for image analysis and an automatic determination and discarding of useless images.

The determination of snow depths for the camera locations was very successful. The collected data is extremely useful to investigate snow accumulation and ablation processes at different time scales (hourly, daily) and for different locations. Furthermore, the data could be used to interpolate the spatial distribution and temporal evolution of a snow cover throughout a mountainous catchment in forested and open areas.

Interception in the forest canopy was calculated qualitatively as a fraction of white pixel within a defined polygon mask in the canopy. In a next step, a method to calculate

[Title Page](#)

[Abstract](#)

[Introduction](#)

[Conclusions](#)

[References](#)

[Tables](#)

[Figures](#)

◀

▶

◀

▶

[Back](#)

[Close](#)

[Full Screen / Esc](#)

[Printer-friendly Version](#)

[Interactive Discussion](#)

quantitative total snow loads from this data will be developed. Another limitation is that the results are dependent on the camera position (angle, distance to the forest). However, the continuous and spatially distributed nature of the observations allows a detailed study of the canopy interception process and snow exposure times for different altitudes and exposures, canopy densities, and meteorological conditions.

Despite some simplifications compared to other approaches (Corripio, 2004; Gorski, 2011) we were able to extract useful data to compare snow surface albedo at different locations by calibrating the data with measured albedo values. The data show realistic values of a high albedo values after a new snowfall, a subsequent decrease in albedo due to snow metamorphism and especially for a melting snow pack with an increasing snow free area.

For the daylight photographs it was possible to identify the state of precipitation and thus the snow line by using the information from the cameras at different altitudes. The information from time-lapse images can also be used to verify snow cover patterns or snow processes simulated from hydrological models (e.g. Farinotti, 2010; Parajka et al., 2012). The spatial and temporal high resolution data collected from a camera network such as the one presented in this study provides a very useful data set which could be used to test assumptions in existing hydrological models and to improve the simulation of the spatio-temporal variability of seasonal snow covers and the related processes at the plot and catchment scale.

## 5 Conclusions

The study highlighted the usefulness of a distributed network of standard digital time-lapse cameras for snow observations in mesoscale mountain catchments. A simple technical modification related to the power supply of the cameras is needed to run the standard digital cameras autonomous at any location in the field. The presented experimental design is an appropriate technique to realize a continuous observation of the spatial distribution and temporal evolution of key aspects of a seasonal snow cover

[Title Page](#)[Abstract](#)[Introduction](#)[Conclusions](#)[References](#)[Tables](#)[Figures](#)[◀](#)[▶](#)[Back](#)[Close](#)[Full Screen / Esc](#)[Printer-friendly Version](#)[Interactive Discussion](#)

<a href="#">Title Page</a>	
<a href="#">Abstract</a>	<a href="#">Introduction</a>
<a href="#">Conclusions</a>	<a href="#">References</a>
<a href="#">Tables</a>	<a href="#">Figures</a>
<a href="#"></a>	<a href="#"></a>
<a href="#">Back</a>	<a href="#">Close</a>
<a href="#">Full Screen / Esc</a>	
<a href="#">Printer-friendly Version</a>	
<a href="#">Interactive Discussion</a>	

throughout a mesoscale catchment. The method is easy to accomplish, low-cost and provides useful data about snow depth and snow albedo as well as important snow processes such as snow interception and state of precipitation. Furthermore, the spatially distributed design of the camera network provides reliable continuous information for the identification of the snow line during winter precipitation events and the interpretation of snowmelt runoff hydrographs. The time-lapse cameras could also be used for other application where visible information could provide useful information of its own or together with additional observations.

**Acknowledgements.** We would like to thank the German Science Foundation (DFG) for the funding of the project “Field Observations and Modelling of Spatial and Temporal Variability of Processes Controlling Basin Runoff during Rain on Snow Events”. We would also like to thank our field assistants Franziska Zieger, Daniel Günther and Denis Blümel for their valuable help in the field and the technicians of the institute Emil Blattmann and Lukas Neuhaus.

## References

- Corripi, J. G.: Snow surface albedo estimation using terrestrial photography, *Int. J. Remote Sens.*, 25, 5705–5729, 2004.
- Farinotti, D., Magnusson, J., Huss, M., and Bauder, A.: Snow accumulation distribution inferred from time-lapse photography and simple modeling, *Hydrol. Process.*, 24, 2087–2097, 2010.
- Floyd, W. and Weiler, M.: Measuring snow accumulation and ablation dynamics during rain-on-snow events: innovative measurement techniques, *Hydrol. Process.*, 22, 4805–2097, 2008.
- Garen, D. C. and Marks, D.: Spatially distributed energy balance snowmelt modeling in a mountainous river basin: estimation of meteorological inputs and verification of model results, *J. Hydrol.*, 315, 126–153, 2005.
- Gorski, K. M.: Albedo project, available at: <https://sites.google.com/site/albedoproject/home> (last access: 19 September 2012), 2011.
- Gray, D. M. and Landine, P. G.: Albedo model for shallow prairie snowcovers, *Can. J. Earth Sci.*, 24, 1760–1768, 1987.
- Hardy, J., Melloh, R., Robinson, P., and Jordan, R.: Incorporating effects of forest litter in a snow process model, *Hydrol. Process.*, 14, 3227–3237, 2000.

- Hedstrom, N. R. and Pomeroy, J. W.: Measurements and modelling of snow interception in the boreal forest, *Hydrol. Process.*, 12, 1611–1625, 1998.
- Hinkler, J., Pedersen, S. B., Rasch, M., and Hansen, B. U.: Automatic snow cover monitoring at high temporal and spatial resolution, using images taken by a standard digital camera, *Int. J. Remote Sens.*, 23, 4669–4682, 2002.
- 5 Jonas, T., Marty, C., and Magnusson, J.: Estimating the snow water equivalent from snow depth measurements in the Swiss Alps, *J. Hydrol.*, 378, 161–167, 2009.
- Jost, G., Weiler, M., Gluns, D. R., and Alila, Y.: The influence of forest and topography on snow accumulation and melt at the watershed-scale, *J. Hydrol.*, 347, 101–115, 2007.
- 10 Jost, G., Moore, R. D., Weiler, M., Gluns, D. R., and Alila, Y.: Use of distributed snow measurements to test and improve a snowmelt model for predicting the effect of forest clear-cutting, *J. Hydrol.*, 376, 94–106, 2009.
- Link, T. and Marks, D.: Point simulation of seasonal snowcover dynamics beneath boreal forest canopies, *J. Geophys. Res.*, 104, 841–857, 1999.
- 15 Lundberg, A. and Koivusalo, H.: Estimating winter evaporation in boreal forests with operational snow course data, *Hydrol. Process.*, 17, 1479–1493, 2003.
- Marsh, P.: Snowcover formation and melt: recent advances and future prospects, *Hydrol. Process.*, 13, 2117–2134, 1999.
- Mazurkiewicz, A. B., Callery, D. G., and McDonnell, J. J.: Assessing the controls of the snow 20 energy balance and water available for runoff in a rain-on-snow environment, *J. Hydrol.*, 354, 1–14, 2008.
- Melloh, R. H., Hardy, J. P., Davis, R. E., and Robinson, P. B.: Spectral albedo/reflectance of littered forest snow during the melt season, *Hydrol. Process.*, 15, 3409–3422, 2001.
- Parajka, J., Haas, P., Kirnbauer, R., Jansa, J., and Blöschl, G.: Potential of time-lapse photography of snow for hydrological purposes at the small catchment scale, *Hydrol. Process.*, online 25 first: doi:10.1002/hyp.8389, 2012.
- Pomeroy, J. W. and Gray, D. M.: Snowcover accumulation in cold climate forests, *Hydrol. Process.*, 16, 3543–3558, 1995.
- Pomeroy, J. W., Shook, K. R., Toth, B., Essery, R. L. H., Pietroniro, A., and Hedstrom, N.: An 30 evaluation of snow accumulation and ablation for land surface modelling, *Hydrol. Process.*, 12, 2339–2367, 1998.

## Applying a time-lapse camera network to observe snow processes

J. Garvelmann et al.

[Title Page](#)

[Abstract](#)

[Introduction](#)

[Conclusions](#)

[References](#)

[Tables](#)

[Figures](#)

◀

▶

◀

▶

[Back](#)

[Close](#)

[Full Screen / Esc](#)

[Printer-friendly Version](#)

[Interactive Discussion](#)

Applying  
a time-lapse camera  
network to observe  
snow processes

J. Garvelmann et al.

Title Page

Abstract

Introduction

Conclusions

References

Tables

Figures

◀

▶

◀

▶

Back

Close

Full Screen / Esc

Printer-friendly Version

Interactive Discussion



- Pomeroy, J. W., Gray, D. M., Brown, T., Hedstrom, N. R., Quinton, W. L., Granger, R. J., and Carey, S. K.: The cold regions hydrological model: a platform for basing process representation and model structure on physical evidence, *Hydrol. Process.*, 21, 2650–2667, 2007.
- Storck, P., Lettenmaier, P. D., and Bolton, S. M.: Measurement of snow interception and canopy effects on snow accumulation and melt in a mountainous maritime climate, Oregon, United States, *Water Resour. Res.*, 38, 1–16, 2002.
- Stottlemyer, R. and Troendle, C. A.: Effect of canopy removal on snowpack quantity and quality, Fraser Experimental Forest, Colorado, *J. Hydrol.*, 245, 165–176, 2001.
- Warren, S. G. and Wiscombe, W. J.: A model for the spectral albedo of snow, II: Snow containing atmospheric aerosols, *J. Atmos. Sci.*, 37, 2734–2745, 1980.
- Winkler, R. D., Splitthouse, D. L., and Golding, D. L.: Measured differences in snow accumulation and melt among clearcut, juvenile and mature forests of Southern British Columbia, *Hydrol. Process.*, 19, 51–62, 2005.
- Wiscombe, W. J. and Warren, S. G.: A model for the spectral albedo of snow, I: pure snow, *J. Atmos. Sci.*, 37, 2712–2733, 1980.

5

10

15

# Applying a time-lapse camera network to observe snow processes

J. Garvelmann et al.

Title Page

## Abstract

Introduction

## Conclusions

## References

## Tables

Figures

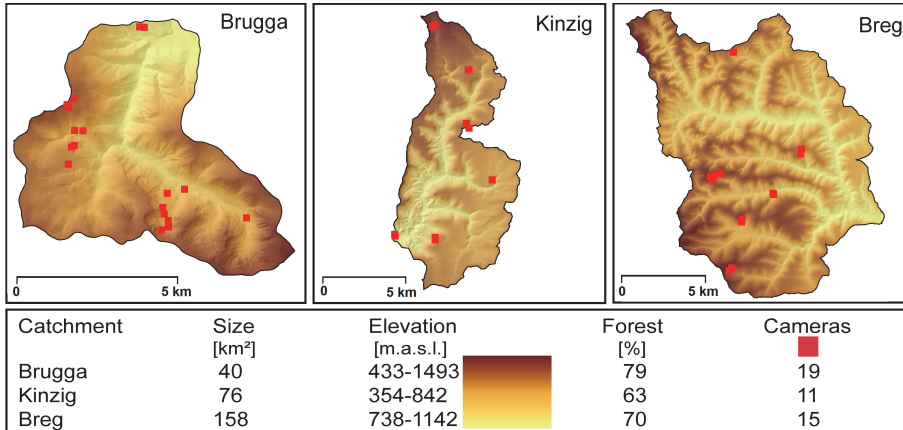


**Fig. 1.** Study catchments in the Black Forest, South-West Germany.



**Fig. 2.** Camera setup used in the presented study.

## Applying a time-lapse camera network to observe snow processes

J. Garvelmann et al.

[Title Page](#)

[Abstract](#)

[Introduction](#)

[Conclusions](#)

[References](#)

[Tables](#)

[Figures](#)

◀

▶

◀

▶

[Back](#)

[Close](#)

[Full Screen / Esc](#)

[Printer-friendly Version](#)

[Interactive Discussion](#)

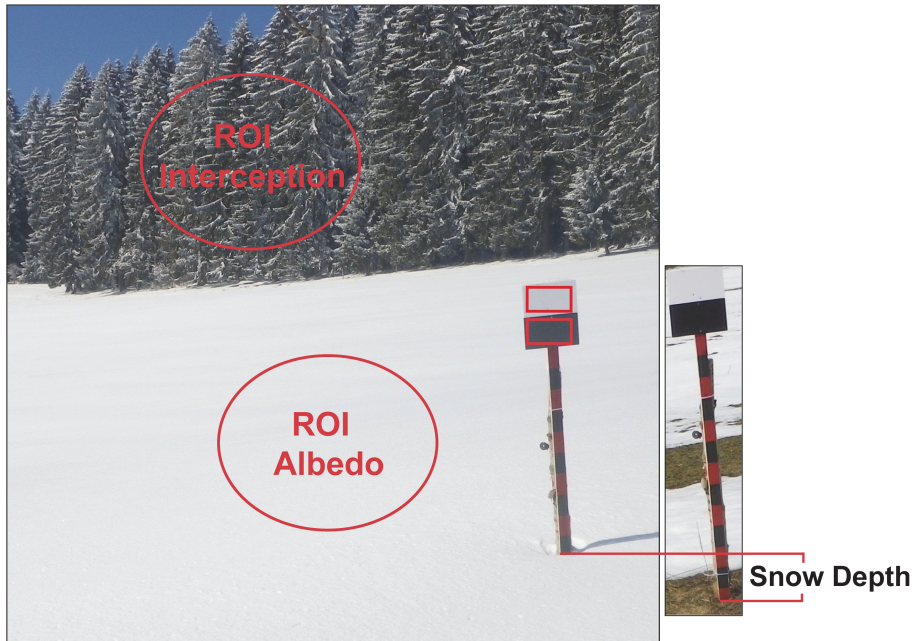


**Fig. 3.** Methodology used for the image processing.

# Applying a time-lapse camera network to observe snow processes

J. Garvelmann et al.

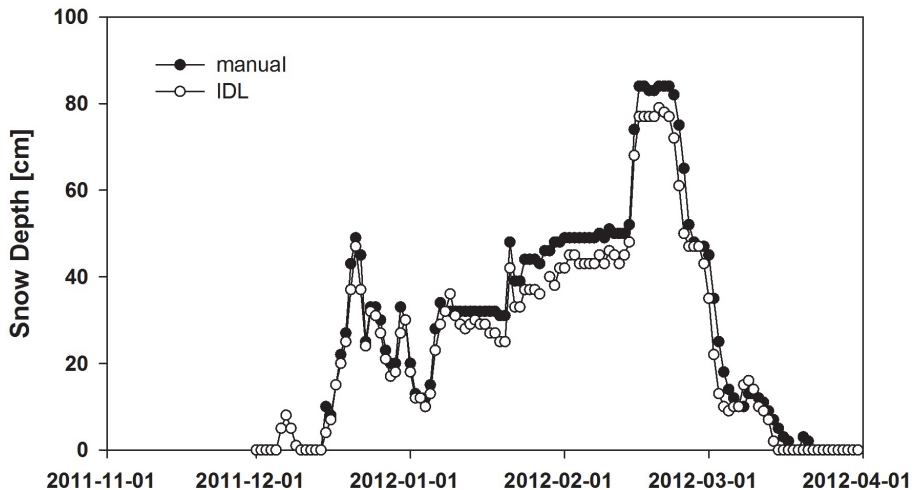


**Fig. 4.** Comparison between manually derived snow depths and the results from an automated IDL routine.

Title Page	
Abstract	Introduction
Conclusions	References
Tables	Figures
◀	▶
◀	▶
Back	Close
Full Screen / Esc	
Printer-friendly Version	
Interactive Discussion	

Applying  
a time-lapse camera  
network to observe  
snow processes

J. Garvelmann et al.

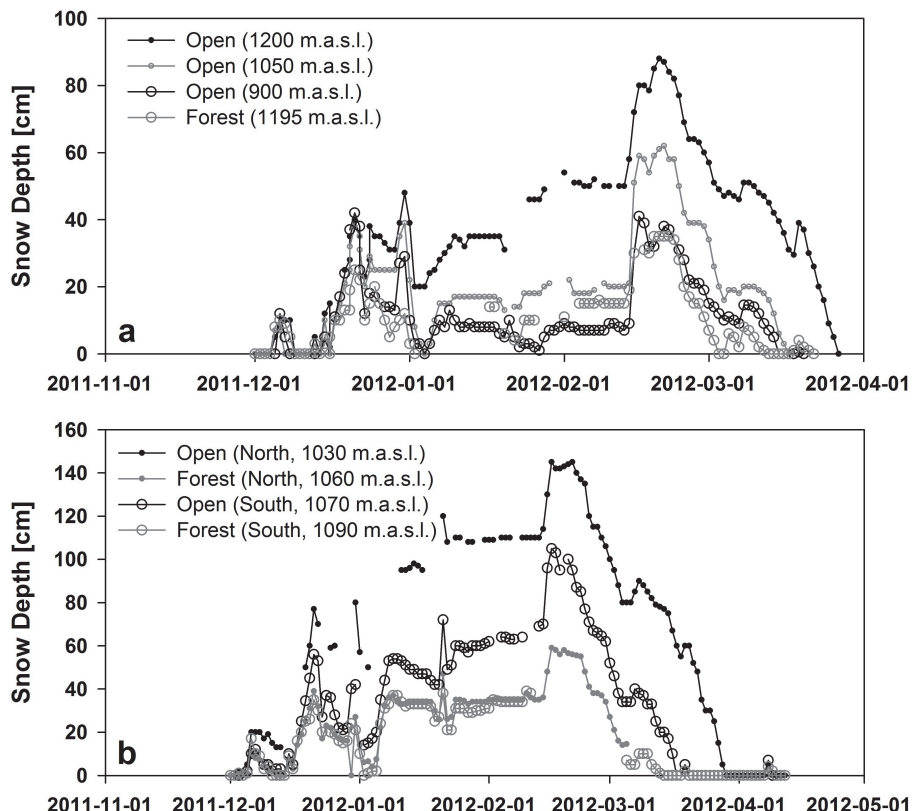


**Fig. 5.** Snow depths dynamics in the winter season 2011/2012 derived from the digital images.

Applying  
a time-lapse camera  
network to observe  
snow processes

J. Garvelmann et al.

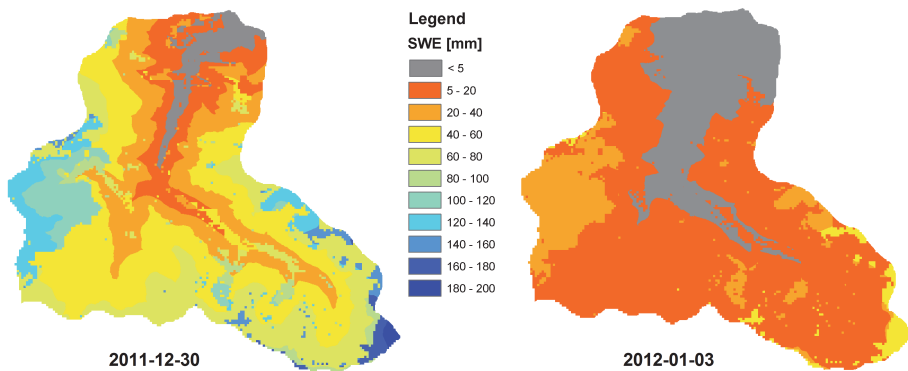


**Fig. 6.** SWE distribution in the Brugga catchment based on the snow depths derived from 19 camera locations and a simple linear regression model for forested and open areas before and after a rain-on-snow flood event on 2 January 2012.

- [Title Page](#)
- [Abstract](#) [Introduction](#)
- [Conclusions](#) [References](#)
- [Tables](#) [Figures](#)
- [◀](#) [▶](#)
- [◀](#) [▶](#)
- [Back](#) [Close](#)
- [Full Screen / Esc](#)
- [Printer-friendly Version](#)
- [Interactive Discussion](#)

## Applying a time-lapse camera network to observe snow processes

J. Garvelmann et al.

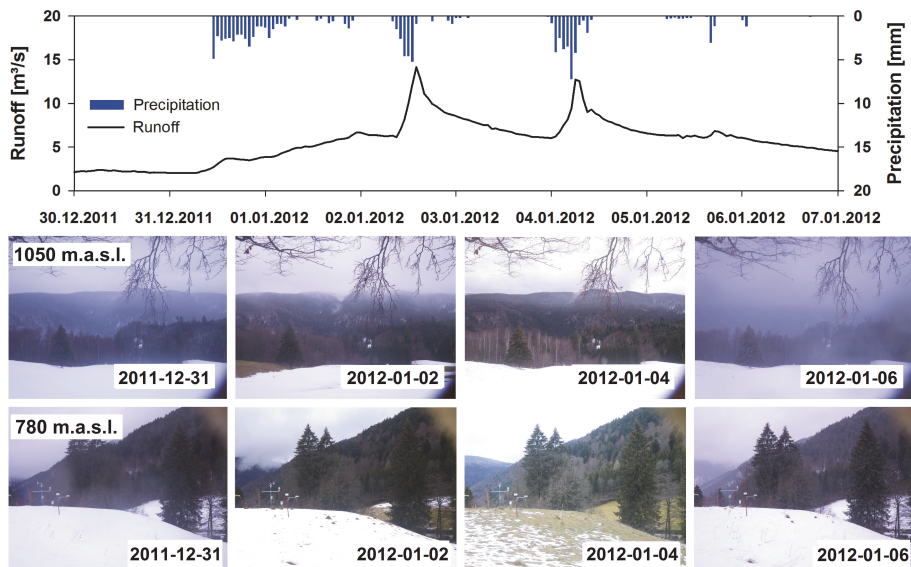


**Fig. 7.** Hydrograph, precipitation and time lapse photographs for the Brugga basin for three runoff events at the beginning of January 2012.

[Title Page](#)

[Abstract](#)

[Introduction](#)

[Conclusions](#)

[References](#)

[Tables](#)

[Figures](#)

◀

▶

◀

▶

[Back](#)

[Close](#)

[Full Screen / Esc](#)

[Printer-friendly Version](#)

[Interactive Discussion](#)

## Applying a time-lapse camera network to observe snow processes

J. Garvelmann et al.

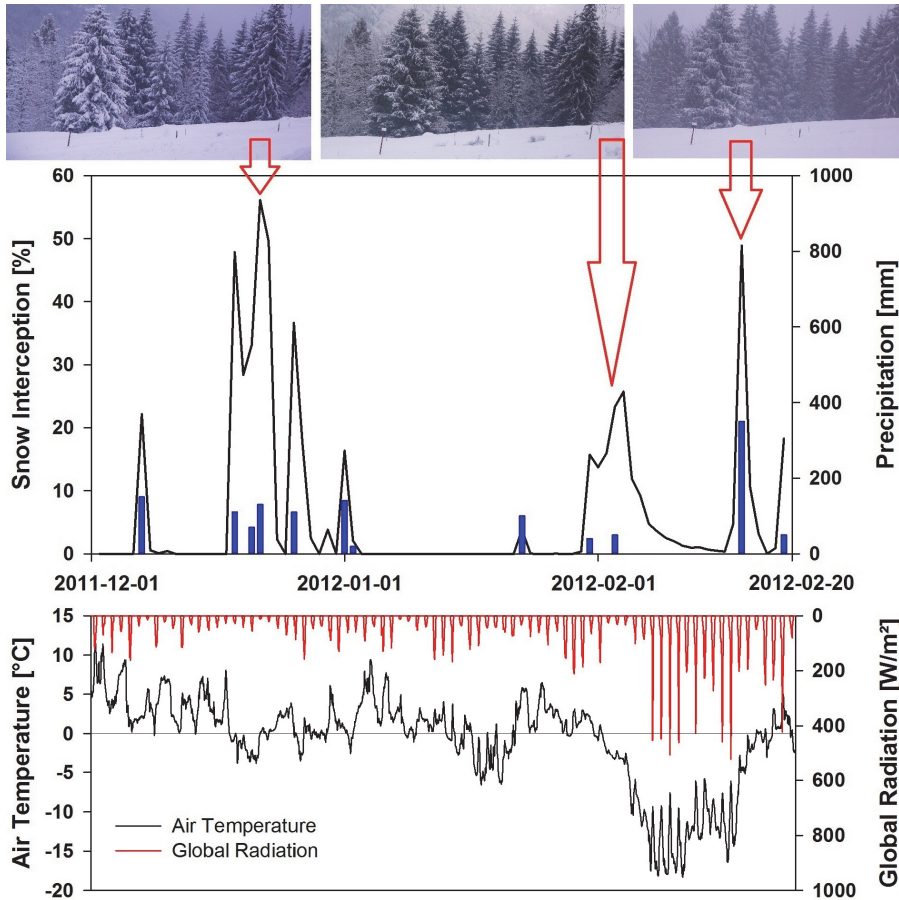


**Fig. 8.** Interception of snow in a conifer forest canopy observed during different snow fall events in winter 2011/2012 with measured air temperature and incoming solar radiation.

# Applying a time-lapse camera network to observe snow processes

J. Garvelmann et al.

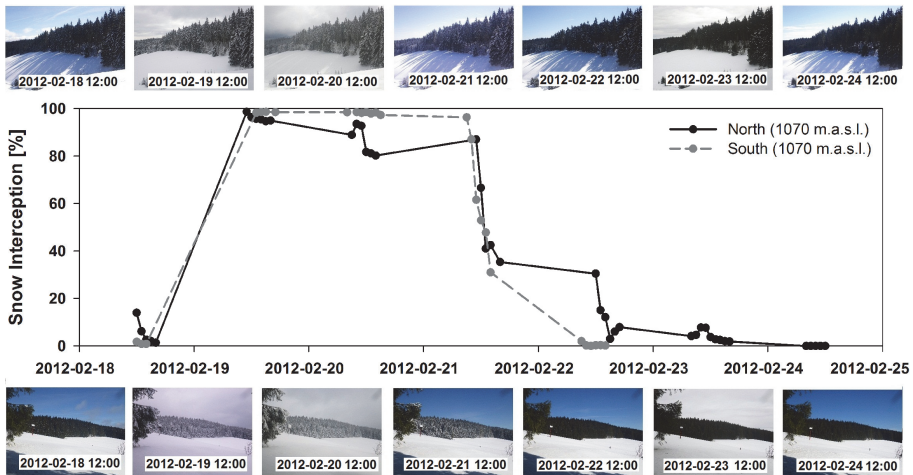


**Fig. 9.** Snow interception in the conifer forest canopy of a north facing and a south facing slope, respectively.

	Title Page
	Abstract
	Introduction
	Conclusions
	References
	Tables
	Figures
	◀
	▶
	◀
	▶
	Back
	Close
	Full Screen / Esc
	Printer-friendly Version
	Interactive Discussion
per	
Discussion Paper	
Discussion Paper	

# Applying a time-lapse camera network to observe snow processes

J. Garvelmann et al.

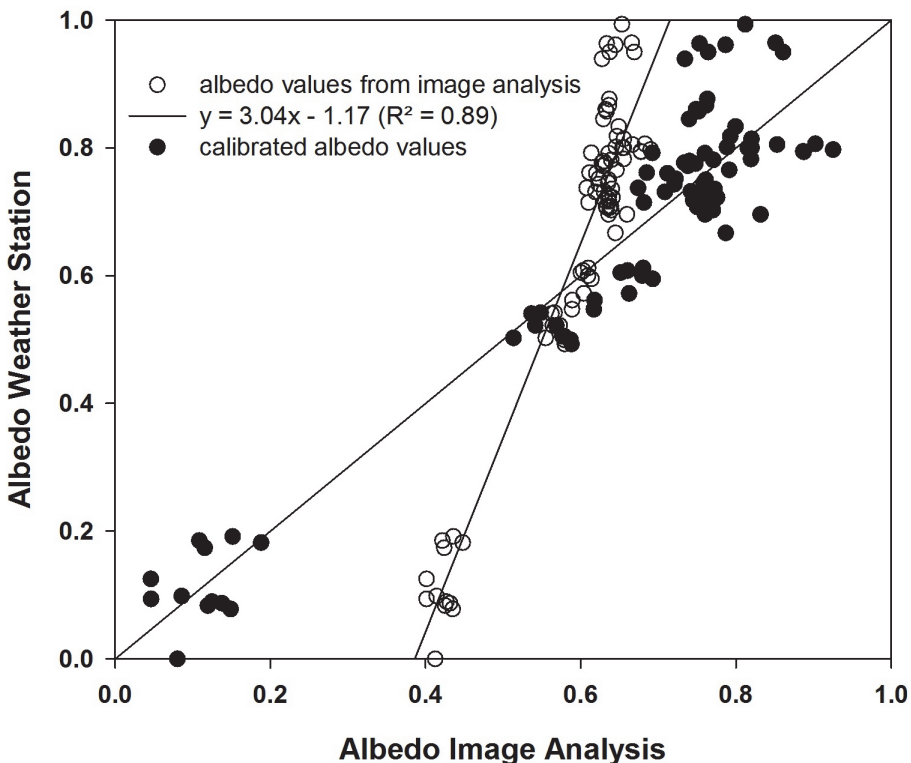


**Fig. 10.** Albedo values measured at the weather station versus albedo values derived from the image analysis.

10714

# Applying a time-lapse camera network to observe snow processes

J. Garvelmann et al.

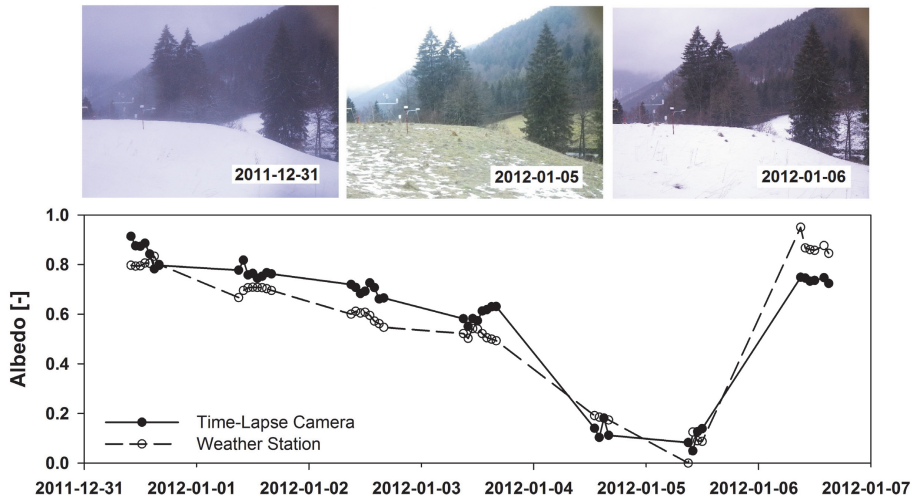


**Fig. 11.** Comparison of calibrated albedo values derived from the image analysis compared to measured albedo values.

Title Page

## Abstract

## Introduction

## usions

## References

Tables

## Figures



Ba

Close

Full Screen / Esc

[Printer-friendly Version](#)

## Interactive Discussion

# Applying a time-lapse camera network to observe snow processes

J. Garvelmann et al.

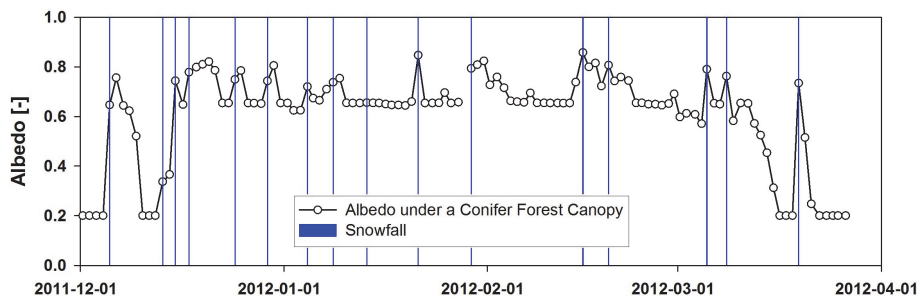


**Fig. 12.** Snow cover albedo under a conifer forest canopy during the winter 2011/2012.

Title Page

## Abstract

## Introduction

## Conclusion

## References

Tables

## Figures



Bac

Close

Full Screen / Esc

[Printer-friendly Version](#)

## Interactive Discussion

# Applying a time-lapse camera network to observe snow processes

J. Garvelmann et al.

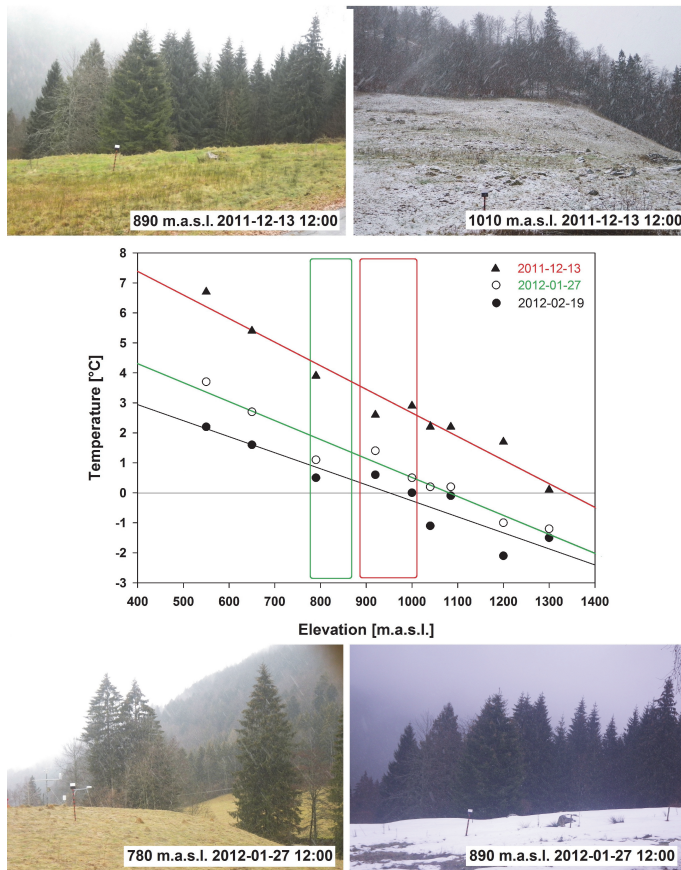


**Fig. 13.** Temperature profiles for different precipitation events in the Brugga catchment. Time-lapse images could be used to determine the state of precipitation.